

# Pulsed TIG Welding–Brazing of Aluminum–Stainless Steel with an Al–Cu Twin Hot Wire

Huan He, Chuansong Wu, Sanbao Lin, and Chunli Yang

(Submitted March 17, 2018; in revised form November 14, 2018; published online January 3, 2019)

A TIG welding–brazing process with a twin aluminum hot wire technique was utilized to control the heat input, improve the joint formation, suppress the interfacial intermetallic compounds (IMCs) and increase the joint strength, thereby creating reliable joints between an aluminum alloy and stainless steel with an ER2319 filler. Twin wires with reasonable diameters and filling modes led to a satisfactory weld of parent metals with varying thicknesses. By the hot wire technique, the reasonable range of the welding current was extended and the thickness of the interfacial IMC at the seam bottom was reduced. In addition, both the tensile strength and stability of the joints increased compared with a cold wire. The IMC consisted of  $\theta$ -(Fe,Cu)<sub>4</sub>Al<sub>13</sub> and minor Cr<sub>0.7</sub>Fe<sub>0.3</sub>Al<sub>6</sub>, and the precipitated phases in the weld were Al<sub>2</sub>Cu and Al<sub>2</sub>CuMg. With an increasing welding current, the IMC thickness significantly increased, while the joint strength decreased. The fracture positions of the joints varied with the corresponding welding currents.

**Keywords** aluminum alloy, intermetallic, stainless steel, TIG welding–brazing, twin hot wire

## 1. Introduction

Welding–brazing techniques, especially arc welding–brazing methods, are promising for joining dissimilar metals such as aluminum/steel because of their flexibility, convenience and cost effectiveness. However, it is difficult to achieve sufficient wetting and spreading of molten aluminum on a steel surface during the joining process. Much research has been performed on this problem, such as utilization of the tandem, the dual-spot laser beam method (Ref 1), the hot wire technique (Ref 2) and coatings including aluminizing, galvanizing (Ref 3) and adding flux (Ref 4). Nevertheless, certain issues still need to be investigated to improve the joint quality of two dissimilar metals in the welding–brazing process.

A more critical problem in joining aluminum to steel is the growth of brittle intermetallic compounds (IMCs), e.g., Fe<sub>3</sub>Al, FeAl, FeAl<sub>2</sub>, Fe<sub>2</sub>Al<sub>5</sub>, FeAl<sub>3</sub> and Fe<sub>4</sub>Al<sub>13</sub>, caused by both chemical reactions and interdiffusion (Ref 5). The most commonly reported IMCs at aluminum–steel joint interfaces are Al-rich IMCs, especially the orthorhombic  $\eta$ -Al<sub>5</sub>Fe<sub>2</sub> and the monoclinic  $\theta$ -Al<sub>13</sub>Fe<sub>4</sub> (Ref 6). The formation of IMCs is necessary for metallurgical bonding between aluminum and

steel, but the growth of IMCs needs to be controlled with respect to both structure and thickness within a reasonable range to avoid brittle and easy-to-crack interfaces.

Control of IMCs is typically achieved by solid-state joining processes including diffusion bonding (Ref 7, 8), magnetic pulse welding (Ref 9), friction welding (Ref 10, 11), friction stir welding (Ref 12, 13) and sometimes certain transition layers (Ref 7, 14, 15). Compared with solid-state welding, it is more difficult to suppress IMCs in electron beam welding (Ref 16), laser welding (Ref 17) and, in particular, arc welding–brazing process (Ref 18–22).

There are three major options for controlling IMCs in the liquid aluminum–solid steel system. The first option is to employ a filler with appropriate alloying elements. The addition of elements including Zn, Si, Mn and Cu to aluminum-based fillers has been proved to be beneficial for controlling the IMCs of Fe–Al interfaces (Ref 23–26). Second, transition metals have been used to suppress the formation of IMCs (Ref 27–29). Finally, heat input adjustment during the welding processes is an effective method for controlling IMCs and improving the joint properties. Heat input reduction achieved by cold metal transfer (CMT) has been proved to be effective in controlling IMCs (Ref 20, 30). A backing block with a higher thermal conductivity has been applied in the aluminum–steel laser welding process to suppress IMCs (Ref 31). Additionally, a combination of laser heating and roll welding has been applied to control IMCs and the properties of aluminum–steel joints (Ref 32). However, in the field of IMC control, there is no systematic research related to the combination of a filler containing the alloying element Cu and heat input adjustment.

In this paper, high-frequency induction twin hot wire technology is proposed for the first time for preheating an Al–Cu filler and adjusting the heat input in pulsed TIG welding–brazing of aluminum–stainless steel. Different wire diameters and filling modes were tested to obtain the acceptable weld formation for different thicknesses of parent metals. In addition, the weld formation, microstructure and mechanical properties of the joints were analyzed and discussed.

**Huan He**, MOE Key Laboratory for Liquid–Solid Evolution and Materials Processing, Institute of Materials Joining, Shandong University, Jinan 250061, China; and State Key Laboratory of Advanced Welding and Joining, Harbin Institute of Technology, Harbin 150006, China; **Chuansong Wu**, MOE Key Laboratory for Liquid–Solid Evolution and Materials Processing, Institute of Materials Joining, Shandong University, Jinan 250061, China; **Sanbao Lin** and **Chunli Yang**, State Key Laboratory of Advanced Welding and Joining, Harbin Institute of Technology, Harbin 150006, China. Contact e-mail: welderhehuan@yahoo.com.

## 2. Materials and Methods

The parent materials employed were a 3.0-mm-thick 5A06 aluminum alloy and SUS321 stainless steel sheets. The filler was an ER2319 aluminum welding wire with a diameter of 1.6 mm. The chemical compositions of the base and filler metals are listed in Table 1. A modified flux (KAlF<sub>4</sub> + Al powder) was employed in the experiments.

The size of the specimen was 100 mm by 50 mm, with a 45° single V-groove in both the steel and aluminum sides. The plate surfaces were first cleaned by abrasive paper or a scraper and acetone, and then, a flux layer that was approximately 0.2–0.5 mm thick was coated on the grooves as well as on the face and back surfaces of the steel, which were 10 mm wide. Butt TIG welding–brazing experiments on aluminum to steel were carried out using a standard welding source. The welding parameters were an AC square wave of 100 Hz, a 4:1 AC balance, an arc length of 3.0–4.0 mm, a welding speed of 150 mm/min and an argon gas flow rate of 8–10 L/min. A CanRecord 5000 × 2 high-speed camera was used to obtain arc and pool images.

The twin hot wire equipment based on the high-frequency induction technique in this research was composed of an induction heating coil, a ceramic tube, a fixture and a wire guide, as illustrated in Fig. 1. High-frequency induction (0.5–1 MHz in the present study) is a method of heating electrically conductive materials. The flow of the AC current through the coil generated an alternating magnetic field that passed through the workpiece. The alternating magnetic field induced eddy currents that heated the wire (Ref 33). Shielding gas was also essential for protecting the wire from oxidation during the heating process. This equipment was able to heat the aluminum wire to any temperature below 400 °C with a feeding rate of up to 1.5 m/min by adjusting the induction current. When the wire temperature was above 400 °C, the aluminum wire softened and feeding became difficult.

To analyze the thermal cycling curves at the interfaces, MARC FEM software was employed to calculate the temperature field. The element birth and death technique and a general double ellipsoid welding heat source were used. The FEM model was verified by a thermocouple instrument made in house.

After welding, the weld macrostructure, microstructure and IMC composition at the interface were examined using an optical microscope, scanning electron microscope (SEM) equipped with energy dispersive spectrometer (EDS) and x-ray crystallography. Tensile tests were conducted using INSTRON-5569 testing machines, with a loading speed of 0.5 mm/min. All tests were performed in triplicate.

## 3. Results

### 3.1 Effects of Twin Wire Feeding on the Weld Formation

The fluid flow in the welding–brazing pool is unstable and asymmetrical because the two sides of the butt joint are

composed of different metals in different states. One side is solid steel with a layer of flux on its surface, and the other side is liquid aluminum melted by the arc. Therefore, when using a single wire, the weld formation is very sensitive to the wire feeding position and fluctuation. With fluctuation during wire feeding, the molten metal in the pool always flows to one side, resulting in a poor appearance, as shown in Fig. 2.

Twin hot wires with the same or different diameters were used to improve the weld formation in the aluminum–steel welding–brazing process. Since the aluminum requires more energy to melt, a filler with a smaller diameter is preferred on the aluminum side. Different wire diameters and heights (from wire end to groove surface) were matched. There are four possible feeding modes: twin  $\phi 1.2$  mm (same height),  $\phi 1.6 + \phi 1.2$  mm (same height),  $\phi 1.6$  mm (higher) +  $\phi 1.2$  mm (lower) and  $\phi 1.6$  mm (lower) +  $\phi 1.2$  mm (higher), as presented in Fig. 3.

For base metals 2 mm in thickness or smaller, as relatively fewer fillers were needed, the use of twin  $\phi 1.2$  mm fillers was reasonable. If the thicknesses of the parent materials were equal to or larger than 3 mm, a  $\phi 1.6$ -mm wire with a larger height on the steel side enabled stable spreading of the molten filler and protected the steel from overheating from the arc, and a  $\phi 1.2$ -mm wire with a smaller height was easy to melt, and therefore, the base aluminum could be fused well, as shown in Fig. 4. By employing feeding mode (c), as shown in Fig. 3, the molten aluminum filler spread well on the flux-coated steel, and the excellent face and back weld formation was observed for base metals with thicknesses of 3 mm, as shown in Fig. 5.

### 3.2 Effects of a Hot Wire on the Welding Procedures and Joint Strength

To obtain a reliable joint of aluminum and steel with satisfactory appearance and strength, a reasonable range of

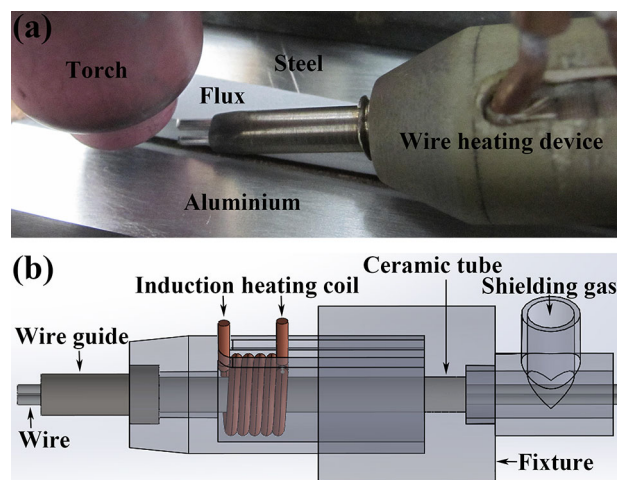


Fig. 1 Schematic of the twin hot wire TIG welding–brazing process, (a) welding–brazing process and (b) twin hot wire system

Table 1 Chemical compositions of the base and filler metals, wt.%

Elements	C	Mn	Mg	Al	Si	Cu	Zn	Ti	Ni	Cr	Fe
SUS321	0.12	2	...	...	1	...	...	0.2	8–10	17–19	Bal.
5A06	...	0.5–0.8	5.8–6.8	Bal.	0.4	0.1	0.2	0.1	...	...	0.4
ER2319	...	0.2–0.4	0.02	Bal.	0.2	5.8–6.8	0.1	0.1–0.2	...	...	0.3

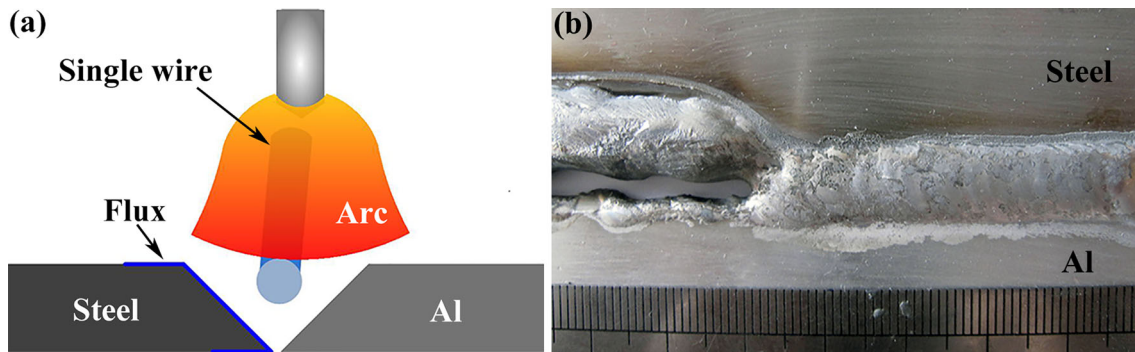


Fig. 2 Schematic of the single wire process and weld formation, (a) single wire process and (b) weld formation

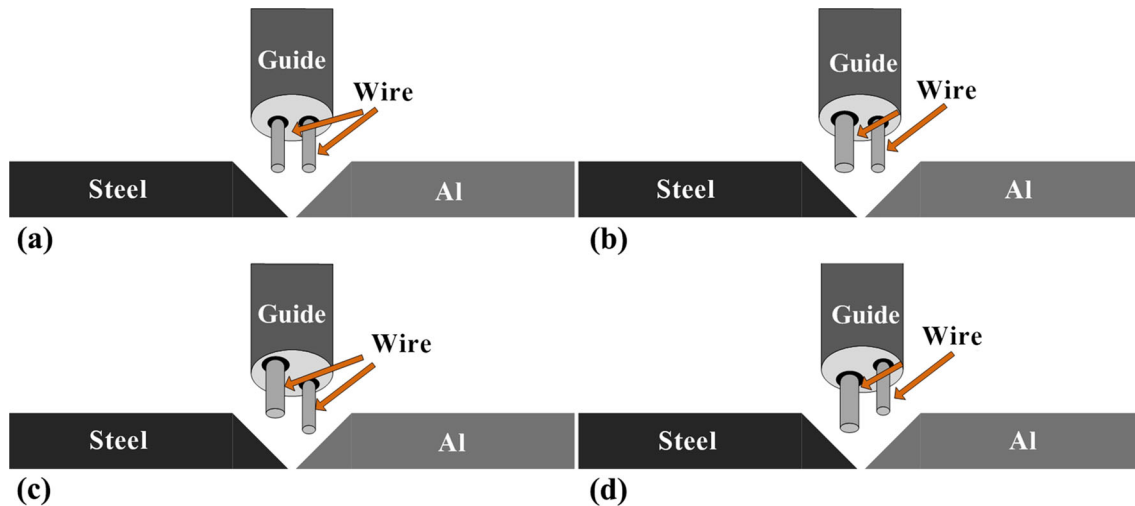


Fig. 3 Schematic of the twin wire diameter and feeding position, (a) twin 1.2 mm (same height), (b) 1.6 mm + 1.2 mm (same height), (c) 1.6 mm (higher) + 1.2 mm (lower) and (d) 1.6 mm (lower) + 1.2 mm (higher)

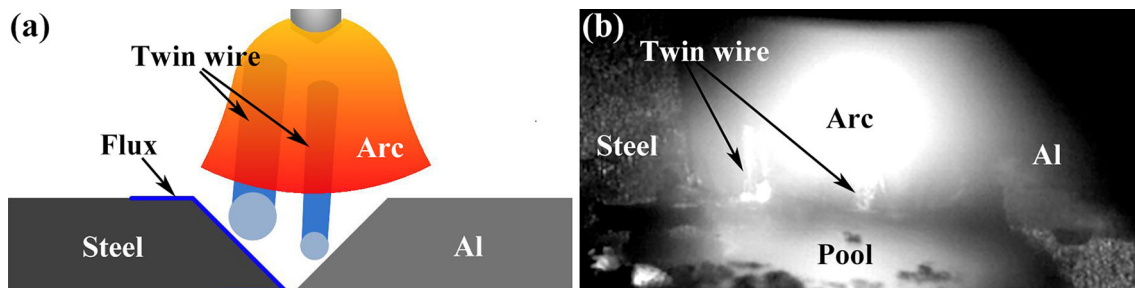


Fig. 4 Schematic of the twin wire welding process, (a) schematic and (b) feeding process

welding current should be adopted to ensure the fusion of the base aluminum and filler without overheating and melting the parent steel. Figure 6 shows a comparison of the welding current ranges under three welding procedures, i.e., a cold wire (20 °C), hot wire (350 °C) and hot wire (350 °C) + pulsed welding current. The hot wire (heating up to 350 °C) combined with pulsed TIG welding can extend the reasonable range of the welding current from 100-120 to 83-120 A, as shown in Fig. 6. The expansion of the welding current window is helpful for achieving a more stable welding–brazing process with lower heat input.

Tensile tests were carried out to evaluate and compare the tensile strengths of the joints in different procedures, and the

results are illustrated in Fig. 7. To demonstrate the trend of tensile strength more clearly, the distributions of the tensile strength were plotted. The cumulative probability in the vertical abscissa was calculated by a mean rank method:

$$P = i / (1 + N) \quad (\text{Eq 1})$$

where  $P$  is the cumulative probability of the measured tensile strength and  $i$  is the order of the total number  $N$  ( $i = 1, 2, 3, \dots, N$ ). All the tensile strength distributions exhibited a linear behavior, indicating a normal probability distribution.

The median of distribution  $S_m$ , located at  $P = 0.5$ , is determined from Fig. 7.  $S_m$  shifted in the positive direction with the hot wire, increasing from 179 MPa with the 20 °C

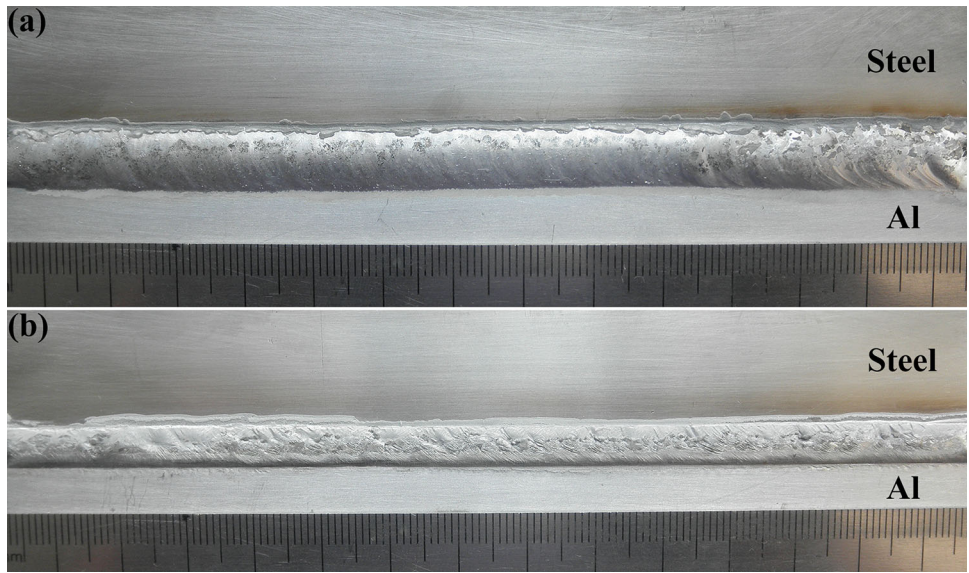


Fig. 5 Welding appearance with a twin wire, (a) face formation and (b) back formation

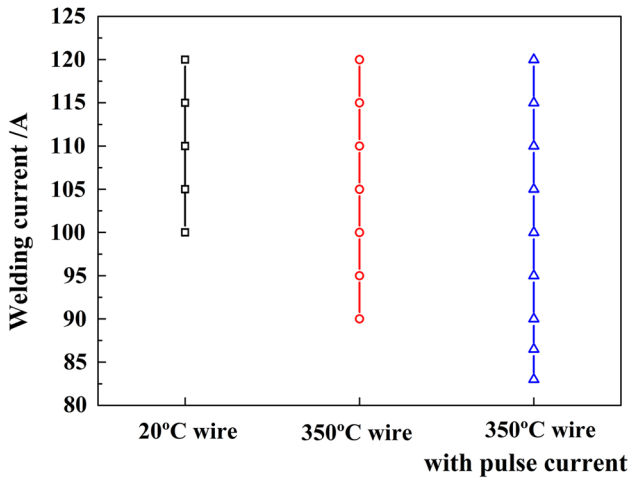


Fig. 6 Welding current ranges for three different procedures

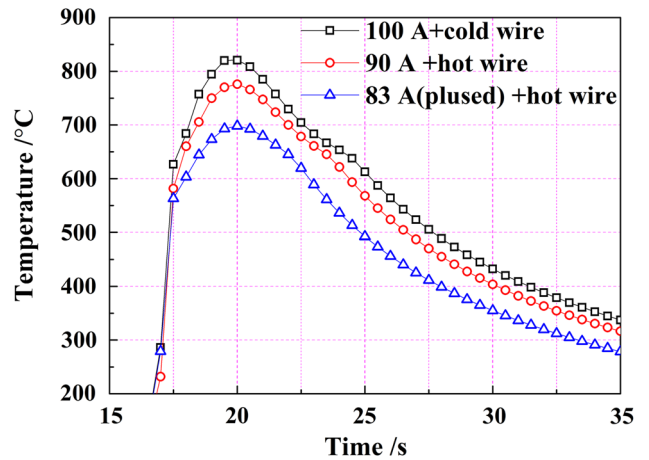


Fig. 8 Thermal cycles at the interfaces under different welding procedures

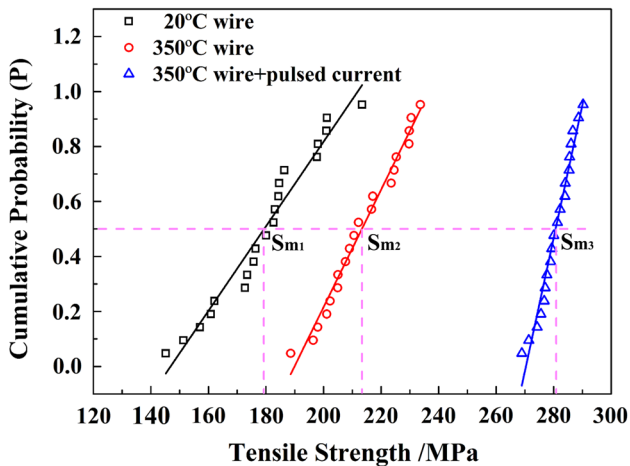


Fig. 7 Strength data distribution of the joints

cold wire to 213 MPa with the 350 °C hot wire and to 280 MPa with the 350 °C hot wire and pulsed TIG welding. Moreover, the strength stability reflected in the slope values significantly improved. The 350 °C hot wire and pulsed welding current increased the joint tensile strength,  $S_m$ , by 56.7% and the strength stability by 215%, compared with those of the cold wire.

Compared with employing a wire at room temperature, using the hot wire at 350 °C not only helped to decrease the minimum welding current from 100 to 83 A but also influenced the temperature field. As shown in Fig. 8, for an 83 A welding current and the 350 °C hot wire, the peak temperature decreased from 820 °C (in the case of the 100 A + cold wire) to 698 °C, and the solid steel–liquid aluminum reaction time decreased from 6.5 to 3.5 s. The decreases in the peak temperature and reaction time indicated a reduced dissolution of steel and therefore a correspondingly thinner IMC.

### 3.3 Macrostructure and Microstructure Analysis

Figure 9(a) presents typical cross-sectional views of the welding–brazing joint with 350 °C hot wire. The aluminum alloy, which had a low melting point, was fused and mixed with the liquid filler metal to produce the welded seam with an obvious fusion line, while the stainless steel remained in the solid state and reacted with liquid aluminum at the interface. Reinforcement at the face and root of the weld was observed. Optical micrographs of different positions in this cross-sectional view are shown in Fig. 9(b), (c) and (d). A visible IMC layer was formed in the steel/welded seam interface (Fig. 9b). Transition phases can be clearly observed in the seam in Fig. 9(c) and (d).

The SEM images, XRD and EDS results of the microstructures are shown in Fig. 10, 11 and Table 2, respectively. Layer I at the interface was identified to be  $\text{Fe}_4\text{Al}_{13}$  based on the EDS and XRD results. It contained certain contents of Cu, Cr and Ni. This result is in good agreement with the TEM results from a previous work (Ref 34). Layer II, with a homogeneity range of 86.3–87.6 at.% Al, had a composition closer to  $\text{Cr}_2\text{Al}_{13}$ ,  $\text{CrAl}_6$  or  $\text{CrAl}_7$  (Ref 35). In the presence of a third metal (Fe, Mn, etc.), the  $\text{CrAl}_6$  phase is known to form another phase with fivefold symmetry and to have a composition corresponding to the chemical formula  $\text{Cr}_{0.7}\text{Fe}_{0.3}\text{Al}_6$  (Ref 36). Similar phases were observed from the interaction of iron-chromium alloys with liquid aluminum (Ref 37). The phases precipitated in the welded seams were  $\text{Al}_2\text{Cu}$  and  $\text{Al}_2\text{CuMg}$  according to the EDS results and previous studies (Ref 23, 38, 39).

### 3.4 Effects of Heat Input on the Microstructures and Properties

Tensile tests were carried out to evaluate the joint tensile strengths that resulted from the use of the 350°C hot wire and different heat inputs. The welding procedures for the different heat inputs were determined by pre-experiments and are listed in Table 3. The results with and without reinforcement are shown in Fig. 12. The tensile strengths of the joints with reinforcement decreased from 280 to 171 MPa and those of the joints without reinforcement were reduced from 185 to 113 MPa when the welding current increased from 83 to 115 A. The presence of reinforcement increased the joint strength by 50%–55%, yet did not influence the strength variation tendencies. Moreover, with the increase in welding current from 83 to 115 A, the IMC thickness significantly increased from 3.3 to 4.9  $\mu\text{m}$ , as shown in Fig. 12(b) and 13.

### 3.5 Fracture Behavior of the Joints

The macrofracture profiles of the joints are shown in Fig. 14. For joints with a high tensile strength (83 A of welding current), the fracture originated from the weld close to fusion zone. On the other hand, for joints with a low tensile strength (110 A of welding current), the fractures evolved from the interfacial IMCs at the bottom of the samples and extended to the weld.

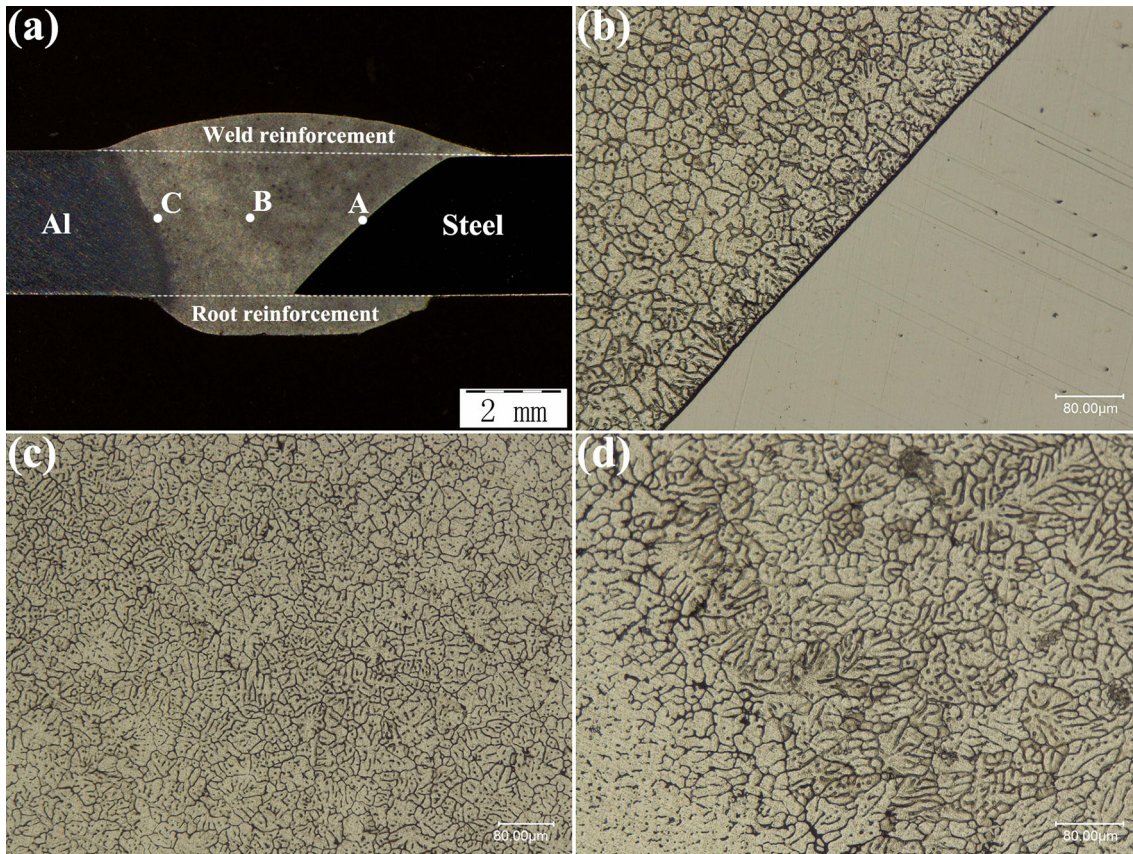


**Fig. 9** Typical transverse cross section and optical micrographs of the aluminum–steel butt joint, (a) typical cross section, (b) optical micrograph of position A, (c) optical micrograph of position B and (d) optical micrograph of position C

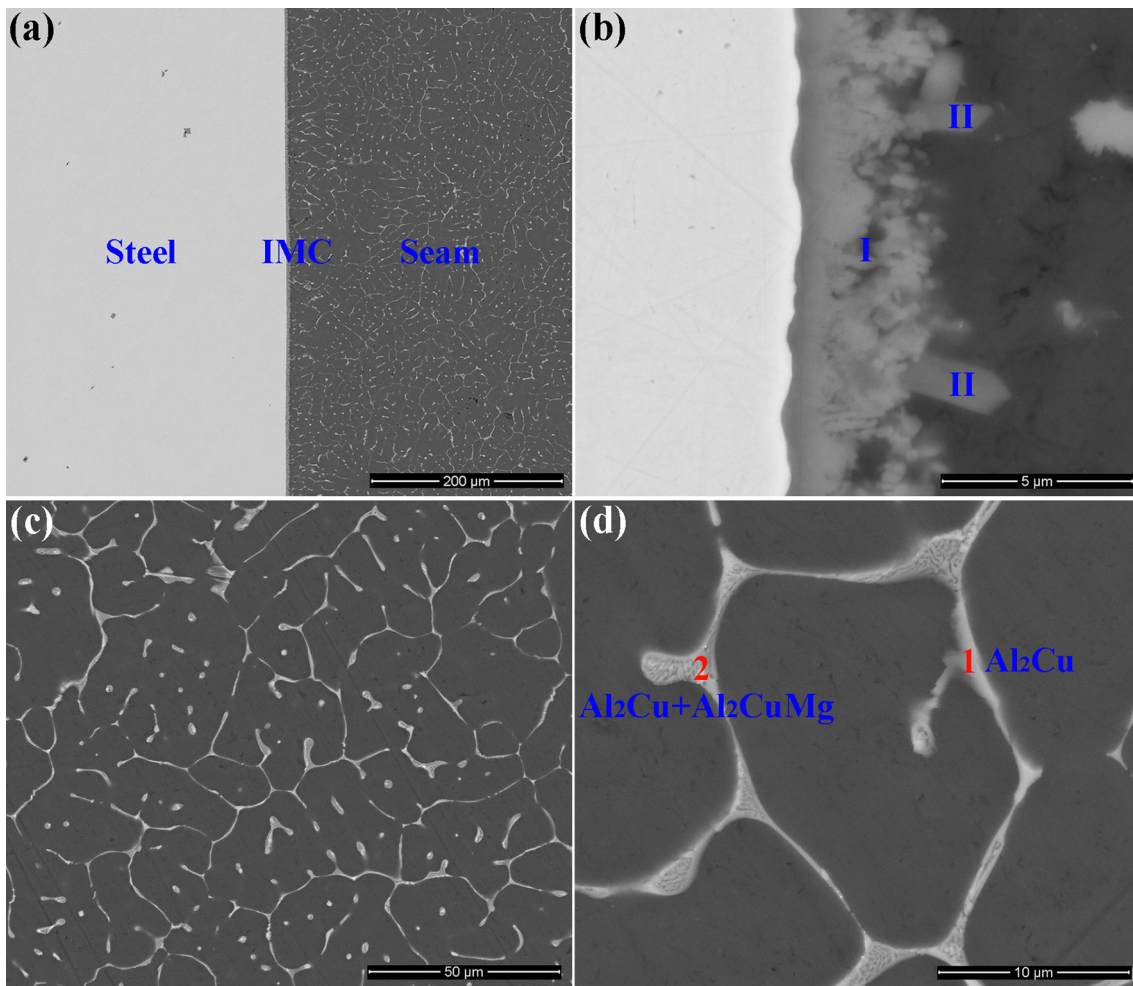


Fig. 10 SEM images of the interface and welded seam, (a) interface, (b) IMC, and (c) and (d) microstructure of the welded seam

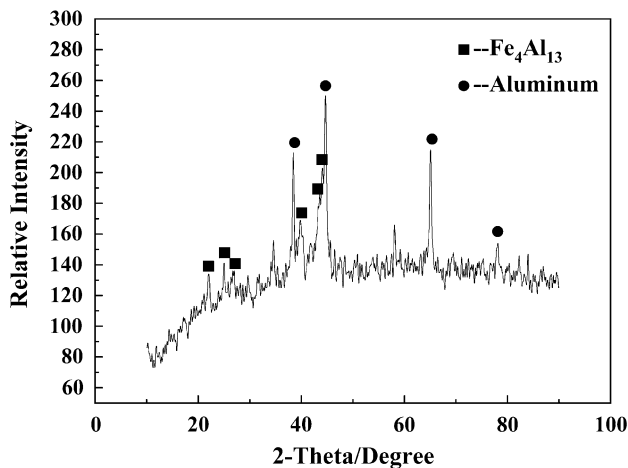


Fig. 11 Micro-x-ray diffraction profile of the interface

## 4. Discussion

The strength of the aluminum–steel welding–brazing joint is affected by many factors, including the weld appearance, groove shape, IMC thickness, structure and composition at the

interface and microstructure of the welded seam. It is critical to discuss the relationships between these factors.

### 4.1 Relationship Among the Weld Appearance, Groove Shape and Joint Strength

Sufficient wetting and stable flow of molten metal are critical for obtaining excellent weld appearances and are achieved in the present work through the use of twin hot wires with various diameters and feeding modes. The application of twin wires can solve the problems of sensitive wire feeding positions and burn-through for thin base metals by adjusting the filling contents at each side. This method can directly expose the seam bottom to the welding arc by converting a sole-centered wire into twin wires at two sides. The centered single wire between the arc and weld bottom is an obstacle to heat transfer. Certain applications of the twin wire method can be found in other processes. For instance, variable polarity plasma arc welding with a twin wire filler has better welding parameter adaptability and a greater permissible assembling gap and offset before welding (Ref 40). The twin wire process produces better quality cladding with less dilution, a smaller heat-affected zone (HAZ) and less distortion (Ref 41). However, this is the first time that the twin wire method has been combined with the hot wire technique and applied to the welding–brazing process of dissimilar metals.

**Table 2** EDS analysis results of IMCs in interfaces and precipitated phase in welded seam, at.%

	Al	Fe	Cr	Ni	Cu	Mg
IMC (I)	74.86	17.50	3.54	1.90	2.20	...
IMC (II)	86.85	4.10	7.02	0.53	1.51	...
Point 1 in welded seam	67.80	0.71	0.37	0.85	30.37	...
Point 2 in welded seam	72.96	0.69	...	...	13.02	13.33

**Table 3** Welding parameters

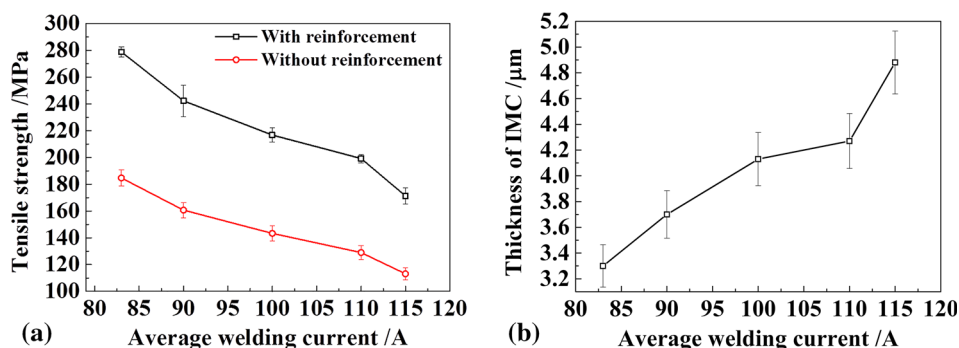
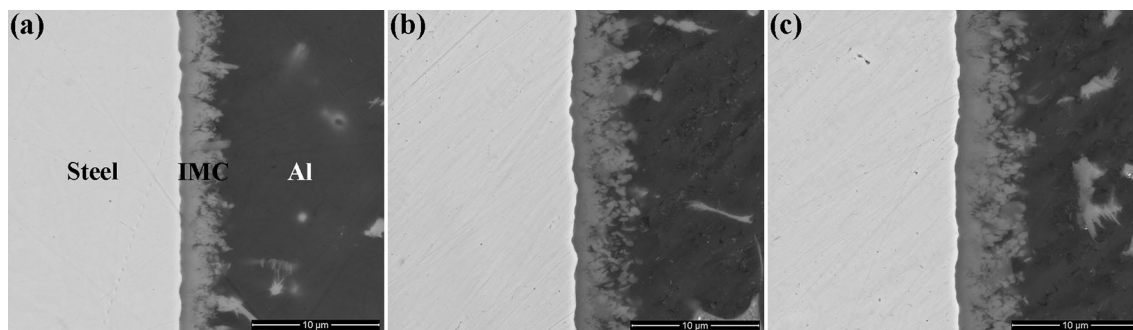
No.	Peak current, A	Pulse on time, %	Basic current, A	Frequency, Hz	Average current, A
1	130	40	52	4	83.2
2	140	40	56	4	89.6
3	140	50	60	4	100
4	150	50	70	4	110
5	150	60	62	4	115

The optimal welding–brazing appearance of aluminum–steel welds always has face and root reinforcement (Ref 42, 43). The existence of the reinforcement increases the joint thickness and enlarges the brazing area. These two aspects both positively impact the joint strength. Furthermore, a reasonable groove shape is critical for obtaining desirable face and root reinforcements (Ref 44). In this work, a 45° half V-shape groove is employed on the steel side. If the groove angle is too small, the filler at the joint root cannot absorb sufficient heat to become molten and flow well, which results in the poor back weld formation. However, if the groove angle is too wide, the filler spreads inadequately on the face surface, which is similar to the

undercutting defect in the fusion welding process. The V-shape of the groove also increases the interface area. Therefore, appropriate reinforcement and grooves are beneficial to joint strength.

#### 4.2 Relationship Between the Welding Current and IMC Thickness

Many researchers have reported that the IMC thickness increases with increasing heat input in many welding processes, including arc welding–brazing (Ref 22, 45, 46), laser welding–brazing (Ref 47, 48) and electron beam welding (Ref 49). These

**Fig. 12** Relationships among the welding current, joint strength and IMC thickness, (a) tensile strength vs. welding current and (b) IMC thickness vs. welding current**Fig. 13** IMC thicknesses related to different levels of the welding current, (a) 83 A, (b) 100 A and (c) 110 A

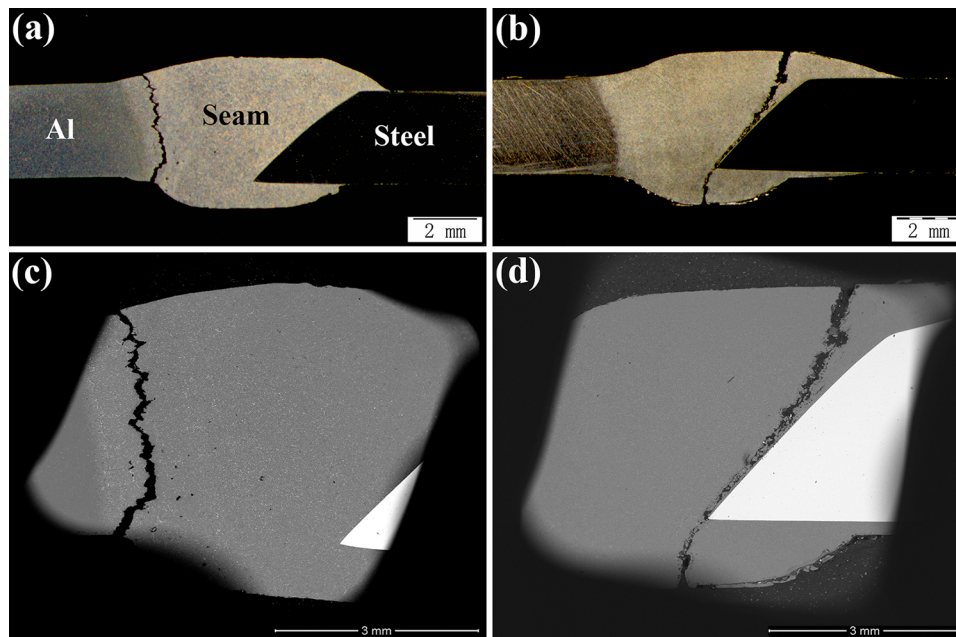


**Fig. 14** Fracture positions of the joints, (a) and (c) 83 A, (b) and (d) 110 A

results agree well with the results presented in this paper. The thickness of IMCs at the brazing interface is mainly determined by the reaction temperature and time for welding aluminum and steel. Higher reaction temperatures and longer reaction times result in larger thicknesses of IMCs (Ref 48). With an increasing heat input, both the peak temperature and the solid–liquid reaction time increase, thickening the IMCs layers and deteriorating the joint’s properties.

#### 4.3 Relationships Among IMCs, Precipitate Phases and Joint Strength

The joint properties are affected by both the IMCs at the brazing interface and the precipitate phases in the welded seam. The IMCs primarily comprise  $\theta$ - $\text{Fe}_4\text{Al}_{13}$  and some  $\text{Cr}_{0.7}\text{Fe}_{0.3}\text{Al}_6$ . However, the effect of the Al–Cr–Fe phase near the IMC on the joint properties is not very clear. The only information that can be obtained is the Vickers hardness of the Al–Cr phase, 5–7 GPa, which is lower than the hardness of  $\text{FeAl}_3$  (8–10 GPa) (Ref 50). The thickness of the IMC is another crucial factor that affects the mechanical properties due to the serious residual stresses caused by the large difference between the coefficients of thermal expansion of the aluminum fillers, IMCs and base steels (Ref 51). Previous research has indicated that 10  $\mu\text{m}$  is the critical value necessary to obtain acceptable joint strength (Ref 52). However, critical values of 3–5  $\mu\text{m}$  for joints of aluminum and steel have been found according to the results in this paper and other published works (Ref 23, 42, 53).

Alloying elements also influence the properties of IMCs and affect the joints. Although Si is considered to be the most effective element for promoting the wetting of molten aluminum on solid steel and reducing the IMC thickness (Ref 4, 54), previous work revealed that a joint of aluminum and stainless steel with an Al–6%Cu filler metal presented higher crack resistance than that with an Al–Si filler (Ref 34). The addition of Cu can effectively decrease the solubility and dissolution rates of Fe in molten aluminum and improve the

tensile properties of  $\text{Al}_{13}\text{Fe}_4$ . Moreover, alloying elements such as Cr and Ni from the stainless steel and Cu from the filler metal may partially replace the iron atoms. Although such replacements do not change the crystal structure of the IMCs (Ref 54, 55), these replacements reduce the hardness of the IMCs and toughen the interfacial structures of joints (Ref 34).

A welding–brazing joint of dissimilar metals is inhomogeneous in terms of its elemental content and internal stress distribution. This type of joint consists of aluminum and steel base metals, IMCs (at the brazing interface), a welding seam and a fusion zone. In this case, the fracture behavior is always complicated. With a 110 A welding current, due to the interfacial stress caused by the increased IMC thickness, a crack originates from the bottom of the IMC. For an 83A welding current, a fracture occurs at the weld close to the fusion zone, which indicates that the area around the IMC interface is not the weakest region. The IMC thickness is compressed to only 3.3  $\mu\text{m}$ . Certain contents of Cu replace the Fe in  $\text{Al}_{13}\text{Fe}_4$ , which significantly reduces the hardness (Ref 23) and contributes to the interface strength. Although Cu promotes a precipitation reaction and the  $\text{Al}_2\text{Cu}$  phase can be abundantly formed to produce high tensile strength at the weld seam, cracks always grow in the grain boundaries of the weld seam due to the interior  $\text{Al}_2\text{Cu}$  phase. An inhomogeneous distribution of two different elements also exists: Mg from the  $\text{AlMg}_6$  in the base metal and Cu from the  $\text{AlCu}_6$  filler in the welded seam near the fusion zone. The inhomogeneous distribution could be another possible reason for the fracture.

## 5. Conclusions

A high-frequency induction twin hot wire technology was successfully developed for TIG welding–brazing of aluminum–stainless steel dissimilar metals. With this system, the weld formation was improved, the welding parameter range was expanded, the heat input and IMC thickness were successfully



controlled, and the strength and stability of the joints significantly increased. The following conclusions can be drawn:

- (1) The problems of thin plates easily experiencing burn-through and the weld formation being sensitive to the position of wire feeding were solved by employing a twin wire feeding system. With different wire combinations and appropriate welding currents, the stable weld formation of joints was achieved when the thicknesses of the base metals were 1.5, 3 and 4 mm. The use of a twin 1.2-mm filler (same height) for the 1.5 mm plate and a 1.6 mm (higher) + 1.2 mm (lower) feeding mode for the 3- and 4-mm plates was the most reasonable for obtaining optimal weld appearance.
- (2) By the hot wire technique, the reasonable range for the welding current was expanded from 100-120 to 83-120 A and the tensile strength of the joints and stability of the joints were increased by 56.7% and 215%, respectively, compared with the cold wire. The heat input was reduced, and the whole temperature field was affected. The maximum temperature in the field changed from 820 °C to 698 °C with a reaction time of 3.5 s, and the thickness of the IMC at the bottom of the interface was approximately 3.3 μm. In this situation, the tensile strength of the joints reached 280 MPa.
- (3) The interfacial IMCs consisted of primary  $\theta$ -Fe<sub>4</sub>Al<sub>13</sub> and minor Cr<sub>0.7</sub>Fe<sub>0.3</sub>Al<sub>6</sub>, and the precipitates in the weld were identified as Al<sub>2</sub>Cu and Al<sub>2</sub>CuMg. With the increase in the welding current from 83 to 115 A, the IMC thickness significantly increased from 3.3 to 4.9 μm, while the tensile strength of the joint decreased from 280 to 171 MPa. The fracture positions of the joints varied corresponding to the welding currents. Specifically, for joints with a high tensile strength, the fracture originated from the weld close to the fusion zone; for joints with a low tensile strength, the fractures evolved from the IMCs at the root of the interface and propagated toward the weld.

## Acknowledgments

The authors would like to express their appreciation for the financial support from the National Natural Science Foundation of China (Grant No. 51605263), China Postdoctoral Science Foundation (Grant No. 2016M602137) and Key Technologies R&D Program of Shandong Province (Grant No. 2017GGX30134).

## References

1. K. Saida, H. Ohnishi, and K. Nishimoto, Fluxless Laser Brazing of Aluminium Alloy to Galvanized Steel Using a Tandem Beam-Dissimilar Laser Brazing of Aluminium Alloy and Steels, *Weld. Int.*, 2010, **24**(3), p 161–168
2. A. Mathieu, S. Pontevicci, J. Viala, E. Cicala, S. Matte, and D. Grevey, Laser Brazing of A Steel/Aluminium Assembly with Hot Filler Wire (88% Al, 12% Si), *Mat. Sci. Eng. A*, 2006, **435**, p 19–28
3. H. Zhang and J. Liu, Microstructure Characteristics and Mechanical Property of Aluminium alloy/Stainless Steel Lap Joints Fabricated by MIG Welding-Brazing Process, *Mat. Sci. Eng. A*, 2011, **528**(19-20), p 6179–6185
4. J.L. Song, S.B. Lin, C.L. Yang, G.C. Ma, and H. Liu, Spreading Behavior and Microstructure Characteristics of Dissimilar Metals TIG Welding-Brazing of Aluminum Alloy to Stainless Steel, *Mat. Sci. Eng. A*, 2009, **509**(1-2), p 31–40
5. L. Agudo, D. Eyidi, C.H. Schmaranzer, E. Arenholz, N. Jank, J. Bruckner, and A.R. Pyzalla, Intermetallic FeAl<sub>3</sub>-Phases in a Steel/Al-Alloy Fusion Weld, *J. Mater. Sci.*, 2007, **42**(12), p 4205–4214
6. X. Li, A. Scherf, M. Heilmairer, and F. Stein, The Al-Rich Part of the Fe-Al Phase Diagram, *J. Phase Equilib. Diffus.*, 2016, **37**(2), p 162–173
7. E.R. Naimon, J.H. Doyle, C.R. Rice, D. Vigil, and D.R. Walmsley, Diffusion Welding of Aluminum to Stainless Steel, *Weld. J.*, 1981, **60**(11), p 17–20
8. J.H. Kong, M. Okumiya, Y. Tsunekawa, K.Y. Yun, S.G. Kim, and M. Yoshida, A Novel Bonding Method of Pure Aluminum and SUS304 Stainless Steel Using Barrel Nitriding, *Metall. Mater. Trans. A*, 2014, **45**(10), p 4443–4453
9. H. Yu and Y. Tong, Magnetic Pulse Welding of Aluminum to Steel Using Uniform Pressure Electromagnetic Actuator, *Int. J. Adv. Manuf. Tech.*, 2017, **91**(5-8), p 2257–2265
10. M.B. Uday, M.N. Ahmad Fauzi, H. Zuhailawati, and A.B. Ismail, Advances in Friction Welding Process: a Review, *Sci. Technol. Weld. Join.*, 2010, **15**(7), p 534–558
11. W. Li, A. Vairis, M. Preuss, and T. Ma, Linear and Rotary Friction Welding Review, *Int. Mater. Rev.*, 2016, **61**(2), p 71–100
12. A. Simar and M.-N. Avettand-Fénoël, State of the Art about Dissimilar Metal Friction Stir Welding, *Sci. Technol. Weld. Join.*, 2017, **22**(5), p 389–403
13. T. Debroy and H.K.D.H. Bhadeshia, Friction Stir Welding of Dissimilar Alloys—a Perspective, *Sci. Technol. Weld. Join.*, 2010, **15**(4), p 266–270
14. M. Reddy, S. Rao, and T. Mohandas, Role of Electroplated Interlayer in Continuous Drive Friction Welding of AA6061 to AISI, 304 Dissimilar Metals, *Sci. Technol. Weld. Join.*, 2008, **13**(7), p 619–628
15. G. Zhang, W. Su, J. Zhang, and Z. Wei, Friction Stir Brazing: a Novel Process for Fabricating Al/Steel Layered Composite and for Dissimilar Joining of Al to Steel, *Metall. Mater. Trans. A*, 2011, **42**(9), p 2850–2861
16. F.W. Bach, A. Beniyash, K. Lau, and R. Versemann, Joining of Steel-Aluminium Hybrid Structures with Electron Beam on Atmosphere, *Adv. Mater. Res.*, 2005, **6**, p 143–150
17. P. Wang, X. Chen, Q. Pan, B. Madigan, and J. Long, Laser Welding Dissimilar Materials of Aluminum to Steel: an Overview, *Int. J. Adv. Manuf. Tech.*, 2016, **87**(9), p 3081–3090
18. Y. Zhang, J. Huang, Z. Cheng, Z. Ye, H. Chi, L. Peng, and S. Chen, Study on MIG-TIG Double-Sided Arc Welding-Brazing of Aluminum and Stainless Steel, *Mater. Lett.*, 2016, **172**, p 146–148
19. Y. Shi, G. Zhang, Y. Huang, L. Lu, J. Huang, and Y. Shao, Pulsed Double-Electrode GMAW-Brazing for Joining of Aluminum to Steel, *Weld. J.*, 2014, **93**(6), p 216–224
20. S. Madhavan, M. Kamaraj, and L. Vijayaraghavan, Microstructure and Mechanical Properties of Cold Metal Transfer Welded Aluminium/Dual Phase Steel, *Sci. Technol. Weld. Join.*, 2016, **21**(3), p 194–200
21. G. Qin, Y. Su, X. Meng, and B. Fu, Numerical Simulation on MIG Arc Brazing-fusion Welding of Aluminum Alloy to Galvanized Steel Plate, *Int. J. Adv. Manuf. Tech.*, 2015, **78**(9), p 1917–1925
22. H. Ma, G. Qin, X. Bai, L. Wang, and Z. Liang, Effect of Initial Temperature on Joint of Aluminium Alloy to Galvanized Steel Welded by MIG Arc Brazing-fusion Welding Process, *Int. J. Adv. Manuf. Tech.*, 2016, **86**(9), p 3135–3143
23. S. Lin, J. Song, C. Yang, C. Fan, and D. Zhang, Brazability of Dissimilar Metals Tungsten Inert Gas Butt Welding-brazing between Aluminum Alloy and Stainless Steel with Al-Cu Filler Metal, *Mater. Des.*, 2010, **31**(5), p 2637–2642
24. J. Yang, Y. Li, H. Zhang, W. Guo, and Y. Zhou, Control of Interfacial Intermetallic Compounds in Fe-Al Joining by Zn Addition, *Mat. Sci. Eng. A*, 2015, **645**, p 323–327
25. Y. Su, X. Hua, and Y. Wu, Influence of Alloy Elements on Microstructure and Mechanical Property of Aluminum-Steel Lap Joint Made by Gas Metal Arc Welding, *J. Mater. Process. Tech.*, 2014, **214**(4), p 750–755
26. L.A. Jácome, S. Weber, A. Leitner, E. Arenholz, J. Bruckner, H. Hackl, and A.R. Pyzalla, Influence of Filler Composition on the Microstructure and Mechanical Properties of Steel-Aluminum Joints Produced by Metal Arc Joining, *Adv. Eng. Mater.*, 2009, **11**(5), p 350–358
27. H. Springer, A. Szczepaniak, and D. Raabe, On the Role of Zinc on the Formation and Growth of Intermetallic Phases During Interdiffu-

- sion Between Steel and Aluminium alloys, *Acta Mater.*, 2015, **96**, p 203–211
28. S. Chen, J. Huang, K. Ma, X. Zhao, and A. Vivek, Microstructures and Mechanical Properties of Laser Penetration Welding Joint With/Without Ni-Foil in an Overlap Steel-on-Aluminum Configuration, *Metall. Mater. Trans. A*, 2014, **45**(7), p 3064–3073
  29. S. Chen, Z. Zhai, J. Huang, X. Zhao, and J. Xiong, Interface Microstructure and Fracture Behavior of Single/Dual-beam Laser Welded Steel-Al Dissimilar Joint Produced with Copper Interlayer, *Int. J. Adv. Manuf. Tech.*, 2016, **82**(1-4), p 631–643
  30. B. Mezrag, F. Deschaux-Beaume, and M. Benachour, Control of Mass and Heat Transfer for Steel/Aluminium Joining Using Cold Metal Transfer Process, *Sci. Technol. Weld. Join.*, 2015, **20**(3), p 189–198
  31. R. Borrisutthekul, T. Yachi, Y. Miyashita, and Y. Mutoh, Suppression of Intermetallic Reaction Layer Formation by Controlling Heat Flow in Dissimilar Joining of Steel and Aluminum Alloy, *Mat. Sci. Eng. A*, 2007, **467**(1-2), p 108–113
  32. M. Rathod and M. Kutsuna, Joining of Aluminum Alloy 5052 and Low-carbon Steel by Laser Roll Welding, *Weld. J.*, 2004, **83**(1), p 16–26
  33. S. Zinn and S.L. Semiatin, *Elements of Induction Heating: Design, Control, and Applications*, ASM International, Russell Township, 1988
  34. J. Song, S. Lin, C. Yang, C. Fan, and G. Ma, Analysis of Intermetallic Layer in Dissimilar TIG Welding-Brazing Butt Joint of Aluminium Alloy to Stainless Steel, *Sci. Technol. Weld. Join.*, 2010, **15**(3), p 213–218
  35. J.L. Murray, The Al-Cr (Aluminum-Chromium) System, *J. Phase Equilib.*, 1998, **19**(4), p 367–375
  36. Fvd Woude and P.J. Schurer, A Study of Quasi-crystalline Al-Fe Alloys by Mössbauer-effect Spectroscopy and Diffraction Techniques, *Can. J. Phys.*, 1987, **65**(10), p 1301–1308
  37. K. Barmak and V. Dybkov, Interaction of Iron-chromium Alloys Containing 10 and 25 Mass% Chromium with Liquid Aluminium Part II, Formation of Intermetallic Compounds, *J. Mater. Sci.*, 2004, **39**(13), p 4219–4230
  38. S.C. Wang and M.J. Starink, Precipitates and Intermetallic Phases in Precipitation Hardening Al-Cu-Mg-(Li) Based Alloys, *Int. Mater. Rev.*, 2005, **50**(4), p 193–215
  39. C. Zhang, M. Gao, G. Li, C. Chen, and X. Zeng, Strength Improving Mechanism of Laser Arc Hybrid Welding of Wrought AA 2219 Aluminium Alloy using AlMg5 Wire, *Sci. Technol. Weld. Join.*, 2013, **18**(8), p 703–710
  40. J. Li, Research on Technology of Variable Polarity Plasma Arc Welding with Twin-wire Filler, Master Thesis, Harbin Institute of Technology (2009)
  41. Z. Sun, M. Kuo and D. P. Twin Wire Gas Tungsten Arc Cladding, SIMTech Technical Report (PT/99/004/JT) (1999)
  42. Z. Ye, J. Huang, Z. Cheng, W. Gao, Y. Zhang, S. Chen, and J. Yang, Combined Effects of MIG and TIG Arcs on Weld Appearance and Interface Properties in Al/steel Double-sided Butt Welding-brazing, *J. Mater. Process. Technol.*, 2017, **250**, p 25–34
  43. J. Xue, Y. Li, H. Chen, and Z. Zhu, Effects of Heat Input on Wettability, Interface Microstructure and Properties of Al/steel Butt Joint in Laser-metal Inert-gas Hybrid Welding-brazing, *J. Mater. Process. Technol.*, 2018, **255**, p 47–54
  44. L. Li, H. Xia, C. Tan, and N. Ma, Effect of Groove Shape on Laser Welding-brazing Al to Steel, *J. Mater. Process. Technol.*, 2018, **252**, p 573–581
  45. L. Shao, Y. Shi, J.K. Huang, and S.J. Wu, Effect of Joining Parameters on Microstructure of Dissimilar Metal Joints Between Aluminum and Galvanized Steel, *Mater. Des.*, 2015, **66**, p 453–458
  46. E. Ünel and E. Taban, Properties and Optimization of Dissimilar Aluminum Steel CMT Welds, *Weld. World*, 2017, **61**(1), p 1–9
  47. S. Mecco, S. Ganguly, S. Williams, and N. Mcpherson, Effect of Laser Processing Parameters on the Formation of Intermetallic Compounds in Fe-Al Dissimilar Welding, *J. Mater. Eng. Perform.*, 2014, **23**(9), p 3361–3370
  48. J. Sun, Q. Yan, W. Gao, and J. Huang, Investigation of Laser Welding on Butt Joints of Al/steel Dissimilar Materials, *Mater. Des.*, 2015, **83**, p 120–128
  49. U. Reisgen, C. Otten, and J. Schoenberger, Investigations about the Influence of the Time-temperature Curve on the Formation of Intermetallic Phases During Electron Beam Welding of Steel-Aluminium Material Combinations, *Weld. World*, 2014, **58**(4), p 443–454
  50. V.S. Zolotarevsky, N.A. Belov, and M.V. Glazoff, *Casting Aluminum Alloys*, Elsevier Science, Amsterdam, 2007
  51. Z. Ye, J. Huang, W. Gao, Y. Zhang, Z. Cheng, S. Chen, and J. Yang, Microstructure and Mechanical Properties of 5052 Aluminum Alloy/Mild Steel Butt Joint Achieved by MIG-TIG Double-sided Arc Welding-Brazing, *Mater. Des.*, 2017, **123**, p 69–79
  52. E. Schubert, M. Klassen, I. Zerner, C. Walz, and G. Sepold, Lightweight Structures Produced by Laser Beam Joining for Future Applications in Automobile and Aerospace Industry, *J. Mater. Process. Technol.*, 2001, **115**(1), p 2–8
  53. H. He, S. Lin, C. Yang, C. Fan, and Z. Chen, Combination Effects of Nocolok Flux with Ni Powder on Properties and Microstructures of Aluminum-Stainless Steel TIG Welding-Brazing Joint, *J. Mater. Eng. Perform.*, 2013, **22**(11), p 3315–3323
  54. M. Yan and Z. Fan, Review Durability of Materials in Molten Aluminum Alloys, *J. Mater. Sci.*, 2001, **36**(2), p 285–295
  55. C. Tan, J. Yang, X. Zhao, K. Zhang, X. Song, B. Chen, L. Li, and J. Feng, Influence of Ni Coating on Interfacial Reactions and Mechanical Properties in Laser Welding-brazing of Mg/Ti Butt Joint, *J. Alloys Compd.*, 2018, **764**, p 186–201